Taylor & Francis
Taylor & Francis Group

Static and dynamic quantization in model-based networked control systems

L. A. MONTESTRUQUE*† and P. J. ANTSAKLIS‡

†EmNet, LLC; 12441 Beckley St., Granger, IN 46530, USA
‡Department of Electrical Engineering, University of Notre Dame,
Notre Dame, IN 46556, USA

In this paper the effects of quantization in an important class of networked control systems called model-based networked control systems (MB-NCS) are considered. The MB-NCS architecture uses an explicit model of the plant in the controller in order to reduce the network traffic, while attempting to prevent excessive performance degradation. Sufficient stability conditions for two types of static and a dynamic quantization schemes for MB-NCS are derived. An important feature is that the stability conditions are explicitly expressed in terms of the plant and controller dynamics, the error between the model and the plant parameters, the transmission or update times, the quantization parameters, and a robustness measure of the system to parameter uncertainty. This is important because it allows the design of the controller and network parameters to achieve the desired goals. Examples are used throughout to illustrate the main results.

1. Introduction

A networked control system (NCS) is a control system in which a data network is used as feedback media. NCS is an important area see for example Walsh *et al.* (1999), Nair and Evans (2000), Yook *et al.* (2002) and Networked Control Systems Sessions (2003). Industrial control systems are increasingly using networks as media to interconnect the different components. However, the use of networked control systems poses some challenges. One of the main problems to be addressed when considering a networked control system is the size of bandwidth required by each subsystem. Since each control subsystem must share the same medium the reduction of the individual bandwidth is a major concern. Two ways of addressing this problem are: minimizing the frequency of transfer of information between the sensor and the controller/actuator; or compressing or reducing the size of the data transferred at each transaction. Shared characteristics among popular digital industrial networks are the small transport time and big overhead per packet, thus using

fewer bits per packet has small impact over the overall bit rate. So reducing the rate at which packets are transmitted brings better benefits than data compression in terms of bit rate used. The MB-NCS architecture makes explicit use of knowledge about the plant dynamics to enhance the performance of the system. MB-NCS were introduced in Montestruque and Antsaklis (2002a) (also see Montestruque and Antsaklis (2004).

Previously we have assumed that the network is capable of transporting data with infinite precision. For example, for the state feedback MB-NCS it is assumed that the sensor sends the exact value of the state over the network to the controller/actuator. This is of course not possible with digital networks since the length of each data packet is finite. It was claimed that, since a large portion of standard industrial networks implement a large number of bits available to represent data, the error between the quantized value and the actual value was negligible. Even when this is so, we want to study the effect of these quantization errors on the system stability.

Several results have been published regarding quantization issues in NCS and sampled data problems

*Corresponding author. Email: lmontest@heliosware.com

(Bamieh 1996, Liberzon and Brockett 2000, Nair and Evans 2000a, b, Elia and Mitter 2001, Fagnani and Zampieri 2002, Hespanha *et al.* 2002, Fu 2003, Liberzon 2003a, b, Nair *et al.* 2003 and Ling and Lemmon 2004). Most results attempt to characterize the stability properties of NCS when the number of bits used by each network packet is finite and small. The main thrust for this research is the need to reduce the amount of bandwidth necessitated by a NCS so that a larger amount of NCS can share the network. The goal with MB-NCS is also the reduction of bandwidth, but the design of the MB-NCS first attempts to reduce the bandwidth by reducing the rate at which packets are sent (Montestruque and Antsaklis 2002a). A second step is to further reduce the bandwidth by reducing the number of bits used to transmit each packet. This allows the designer to consider several design parameters in a sequential fashion. Specifically, a stable non-quantized MB-NCS must be designed first using previous results (Montestruque and Antsaklis 2002a). Then, the effect of quantization can be assessed using the results in this paper. In this way the designer has at her disposal a number of parameters that can be modified, namely the packet transmission times and the number of bits used for each packet. Sufficient conditions on the control system stability can be given depending on bounds over the model uncertainty.

In this paper stability conditions for MB-NCS under popular quantization schemes are derived. Both static quantizers and dynamic quantizers are considered. Static quantizers have quantization schemes that do not vary with time, that is the error between the quantized value and the real value does not depend on time. Two quantizers of this type are considered: the uniform quantizer with a constant maximum quantization error; and the logarithmic quantizer with a maximum quantization error that is proportional to the norm of the quantized value. Dynamic quantizers dynamically adjust their quantization regions to compensate for uncertainties while giving a quantization error that shrinks with time.

The main contributions of this paper are the results on stability of quantized MB-NCS that show the explicit dependence on the update time, the control law, the model dynamics, the quantization parameters, and the difference between the model and plant dynamics. In §2 the basic MB-NCS setup is reviewed for completeness. Stability of MB-NCS with no quantization and periodic transmissions are considered. In §3 the stability of MB-NCS with two types of static quantizers are studied, namely the uniform quantizer and the logarithmic quantizer. The stability of MB-NCS with a dynamic quantizer is studied in §4. Conclusions are given in §5.

2. Stability of a state feedback linear MB-NCS

We consider the control of a continuous linear plant where the state sensor is connected to a linear controller/actuator via a network. In this case, the controller uses an explicit model of the plant that approximates the plant dynamics and makes possible the stabilization of the plant even under slow network conditions.

In this section we determine conditions under which the transfer time between the sensor and the controller/actuator results in a stable control system. An approximate model of the plant is used in the controller/actuator side to estimate the actual value of the plant state vector, in this way the sensor can delay the transmission of update information about the plant state. The main idea is to perform the feedback by updating the model's state using the actual state of the plant that is provided by the sensor. The rest of the time the control action is based on a plant model that is incorporated in the controller/actuator and is running open loop for a period of h seconds. The control architecture is shown in figure 1.

Our approach incorporates a model of the plant, the state of which is updated at discrete intervals by the plant's state. We present a necessary and sufficient condition for stability that results in a maximum transfer time.

If all the states are available, then the sensors can send this information through the network to update the model's vector state. Throughout this paper we will assume that the compensated model is stable and that the transportation delay is negligible. We will assume that the frequency at which the network updates the state in the controller is constant. The goal is to find the smallest frequency at which the network must update the state in the controller, that is, an upper bound for h, the update time.
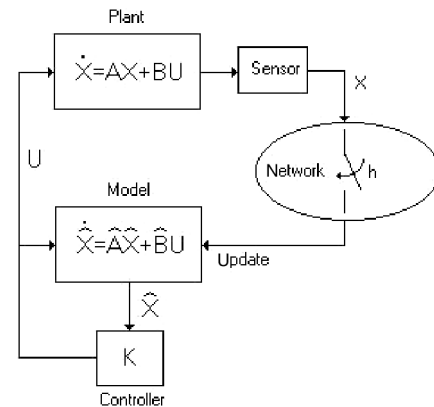
Figure 1. Proposed configuration of networked control system.

Consider the control system of figure 1 where the plant is given by $\dot{x} = Ax + Bu$, the plant model by $\dot{\hat{x}} = \hat{A}\hat{x} + \hat{B}u$, and the controller by $u = K\hat{x}$. The state error is defined as $e = x - \hat{x}$, and represents the differences between the plant state and the model state. The modelling error matrices $\tilde{A} = A - \hat{A}$ and $\tilde{B} = B - \hat{B}$ represent the difference between the plant and the model. Also define the state error $e(t) = x(t) - \hat{x}(t)$ and

$$\Lambda = \begin{bmatrix} A + BK & -BK \\ \tilde{A} + \tilde{B}K & \hat{A} - \tilde{B}K \end{bmatrix}.$$

A necessary and sufficient condition for stability of the state feedback MB-NCS is now presented.

Theorem 1 (Montestruque and Antsaklis 2003): *The State Feedback MB-NCS is globally exponentially stable around the solution $z = [x^T - e^T]^T = 0$ if and only if the eigenvalues of*

$$\begin{bmatrix} I & 0 \\ 0 & 0 \end{bmatrix} e^{\Lambda h} \begin{bmatrix} I & 0 \\ 0 & 0 \end{bmatrix}$$

are strictly inside the unit circle.

It can be shown (Montestruque 2004) that the eigenvalues of

$$M = \begin{bmatrix} I & 0 \\ 0 & 0 \end{bmatrix} e^{\Lambda h} \begin{bmatrix} I & 0 \\ 0 & 0 \end{bmatrix}$$

are inside the unit circle if and only if the eigenvalues of $N = e^{(\hat{A} + \hat{B}K)h} + \Delta(h)$ with $\Delta(h) = e^{Ah} \int_0^h e^{-A\tau} (\tilde{A} + \tilde{B}K) \times e^{(\hat{A} + \hat{B}K)\tau} d\tau$ are inside the unit circle. Observe that the

eigenvalues of the compensated model appear in the first term of N and that the second term $\Delta(h)$ can be made small by having small update times h or small modelling error. A detailed proof for Theorem 1 can be found in Montestruque and Antsaklis (2002a or 2002b).

Example 1: In real applications uncertainty can frequently be expressed as tolerances over the different measured parameter values of the plant. This can be mapped into structured or parametric uncertainties on the state space matrices. Next an example is given on how Theorem 1 can be applied if two entries on the A matrix of the model can vary within a certain interval

$$\text{model: } \hat{A} = \begin{bmatrix} 0 & 0 \\ 0 & 1 \end{bmatrix}, \quad \hat{B} = \begin{bmatrix} 0 \\ 1 \end{bmatrix};$$

$$\text{plant: } A = \begin{bmatrix} 0 & 1 + \tilde{a}_{12} \\ 0 + \tilde{a}_{21} & 0 \end{bmatrix}, \quad B = \begin{bmatrix} 0 \\ 1 \end{bmatrix};$$

$$\text{with } \tilde{a}_{12} = [-0.5, \, 0.5], \quad \tilde{a}_{21} = [-0.5, \, 0.5]$$

$$\text{controller: } K = [-1, \, -2].$$

The system will now be tested for an update time of $h = 2.5$ seconds. The following contour plot in figure 2 represents the maximum eigenvalue magnitude for the test matrix M as a function of the $(1, 2)$ and $(2, 1)$ entries possible values. Here the contours at height equal to one are relevant to stability. It is easy to isolate the stable and unstable regions in the uncertainty parameter plane. The stable region is between the lines labelled as 1.
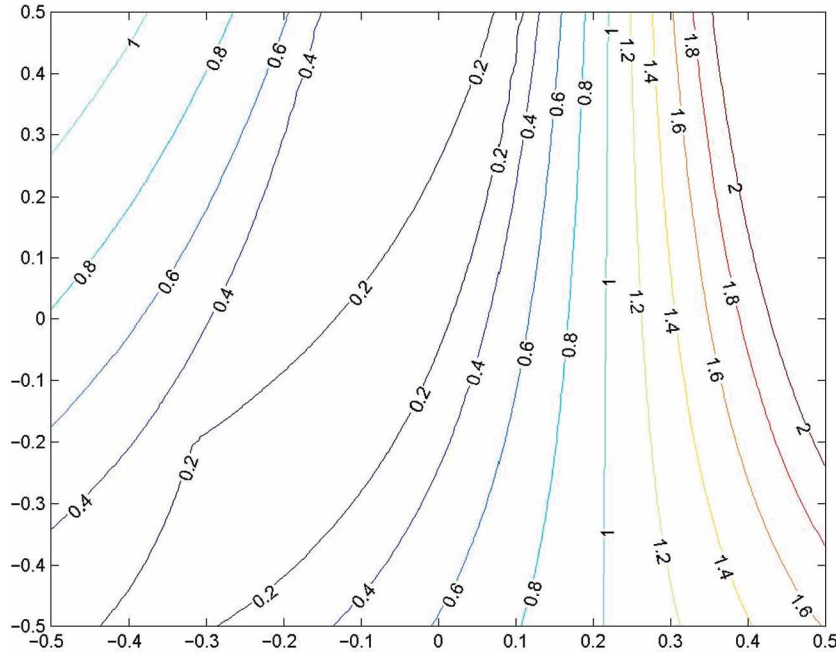
Figure 2. Contour plot maximum eigenvalue magnitude vs model error.

3. Stability of MB-NCS with static quantization

In this section we address the stability analysis of a state feedback MB-NCS using a static quantizer. Static quantizers have defined quantization regions that do not change with time. They are an important class of quantizers since they are simple to implement in either hardware or software and are not as computationally expensive as their dynamic counterparts. Two types of quantizers are analysed here, namely uniform quantizers and logarithmic quantizers. Each quantizer is associated with two popular data representations. The uniform quantizer is associated with the fixed-point data representation. Indeed, fixed-point numbers have a constant maximum error regardless of how close is the actual number to the origin. Logarithmic quantizers on the other hand are associated with floating-point numbers, this allows the maximum error to decrease as the actual number is close to origin.

3.1 *State feedback MB-NCS with uniform quantization*

Let a uniform quantizer be described by a function $q: R^n \to R^n$ with the following property:

$$\|z - q(z)\| \le \delta, \quad z \in R^n, \quad \delta > 0. \quad (1)$$

Theorem 2: *Assume that the networked system without quantization is stable and satisfies*

$$\left(e^{(\hat{A}+\hat{B}K)^T h} + \Delta(h)^T\right) P\left(e^{(\hat{A}+\hat{B}K)h} + \Delta(h)\right) - P = -Q_D \quad (2)$$

with P and Q_D symmetric and positive definite. Then when using the uniform quantizer defined by (1), *the state feedback MB-NCS plant state will enter and remain in the region $\|x\| \le R$ defined by*

$$R = \left(e^{\bar{\sigma}(\hat{A}+\hat{B}K)h} + \Delta_{\max}(h)\right)r + \left(e^{\bar{\sigma}(A)h} + \Delta_{\max}(h)\right)\delta$$

$$\text{where } r = \sqrt{\frac{\lambda_{\max}((e^{Ah} - \Delta(h))^T P(e^{Ah} - \Delta(h))^T)\delta^2}{\lambda_{\min}(Q_D)}}$$

and $\Delta_{\max}(h) = \int_0^h e^{\bar{\sigma}(A)(h-\tau)}\bar{\sigma}(\tilde{A} + \tilde{B}K)e^{\bar{\sigma}(\hat{A}+\hat{B}K)\tau}d\tau$.

Proof: The response for the error is given now by

$$e(t) = e^{A(t-t_k)}e(t_k) + \Delta(t - t_k)\hat{x}(t_k^+)$$

$$= e^{A(t-t_k)}e(t_k) + \Delta(t - t_k)(x_k - e(t_k))$$

$$= \left(e^{A(t-t_k)} - \Delta(t - t_k)\right)e(t_k) + \Delta(t - t_k)x_k \quad (3)$$

where

$$\Delta(t - t_k) = \int_0^{t-t_k} e^{A(t-t_k-\tau)}(\tilde{A} + \tilde{B}K)e^{(\hat{A}+\hat{B}K)\tau}d\tau.$$

Note that since there is non zero quantization error, the initial value for the error $e(t_k)$ is no longer zero as it was in the case for non-quantized MB-NCS. Moreover the contribution due to this initial value for the error will grow exponentially with time and with a rate that corresponds to the uncompensated plant dynamics. So at time $t \in [t_k, t_{k+1}]$ the plant state is

$$x(t) = \hat{x}(t) + e(t)$$

$$= e^{(\hat{A}+\hat{B}K)(t-t_k)}x_k + \left(e^{A(t-t_k)} - \Delta(t - t_k)\right)e(t_k)$$

$$+ \Delta(t - t_k)x_k. \quad (4)$$

We can therefore evaluate a Lyapunov function $V = x^T P x$ at any instant in time $t \in [t_k, t_{k+1}]$. It is known that for uniformly exponential stability we require (Ye *et al.* 1998) that

$$\frac{1}{h}(V(x(t_{k+1})) - V(x(t_k))) \le -c(\|x(t_k)\|^2), c \in R^+. \quad (5)$$

We are interested in the value of the Lyapunov function V at t_{k+1}

$$V(x(t_{k+1})) = x(t_{k+1})^T P x(t_{k+1})$$

$$= x_k^T \left(e^{(\hat{A}+\hat{B}K)h} + \Delta(h)\right)^T P\left(e^{(\hat{A}+\hat{B}K)h} + \Delta(h)\right)x_k$$

$$+ e_k^T (e^{Ah} - \Delta(h))^T P(e^{Ah} - \Delta(h))e_k \quad (6)$$

where

$$h = h_k = t_{k+1} - t_k > 0, \quad e_k = e(t_k).$$

So we obtain

$$V(x(t_{k+1}))V(x(t_k))$$

$$= x_k^T \left(e^{(\hat{A}+\hat{B}K)h} + \Delta(h)\right)^T P\left(e^{(\hat{A}+\hat{B}K)h} + \Delta(h)\right)x_k$$

$$+ e_k^T \left(e^{Ah} - \Delta(h)\right)^T P\left(e^{Ah} - \Delta(h)\right)e_k - x_k^T P x_k$$

$$= e_k^T \left(e^{Ah} - \Delta(h)\right)^T P\left(e^{Ah} - \Delta(h)\right)e_k - x_k^T Q_D x_k. \quad (7)$$

Note that we can compute $e^{Ah} - \Delta(h)$ as follows:

$$e^{Ah} - \Delta(h) = \begin{bmatrix} I & 0 \end{bmatrix} \left(e^{\begin{bmatrix} A & \tilde{A}+\tilde{B}K \\ 0 & \hat{A}+\hat{B}K \end{bmatrix}(t-t_k)}\right) \begin{bmatrix} I \\ -I \end{bmatrix}. \quad (8)$$

We can bound (7) by

$$e_k^T(\mathrm{e}^{Ah} - \Delta(h))^T P(\mathrm{e}^{Ah} - \Delta(h))e_k - x_k^T Q_D x_k$$
$$\leq \lambda_{\max}\big((\mathrm{e}^{Ah} - \Delta(h))^T P(\mathrm{e}^{Ah} - \Delta(h))\big)\delta^2 - \lambda_{\min}(Q_D)||x_k||^2. \tag{9}$$

The sampled value of the state of the plant at the update times will enter the region $||x|| \leq r$ where

$$r = \sqrt{\frac{\lambda_{\max}((\mathrm{e}^{Ah} - \Delta(h))^T P(\mathrm{e}^{Ah} - \Delta(h)))\delta^2}{\lambda_{\min}(Q_D)}}. \tag{10}$$

The plant state vector might exit this region between samples, as pictured in figure 3. The maximum magnitude the state of the plant can reach between samples is given by

$$||x(t)|| = \left\| \big(\mathrm{e}^{(\hat{A}+\hat{B}K)(t-t_k)} + \Delta(t - t_k)\big)x_k \right.$$
$$\left. + \big(\mathrm{e}^{A(t-t_k)} - \Delta(t - t_k)\big)e_k \right\|$$
$$\leq \big(\mathrm{e}^{\bar{\sigma}(\hat{A}+\hat{B}K)h} + \Delta_{\max}(h)\big)r + \big(\mathrm{e}^{\bar{\sigma}(A)h} + \Delta_{\max}(h)\big)\delta \tag{11}$$

where

$$\Delta_{\max}(h) = \int_0^h \mathrm{e}^{\bar{\sigma}(A)(h-\tau)}\bar{\sigma}(\tilde{A} + \tilde{B}K)\mathrm{e}^{\bar{\sigma}(\hat{A}+\hat{B}K)\tau}\mathrm{d}\tau$$

Therefore the plant state will enter and remain in the region $||x|| \leq R$ defined by

$$R = \big(\mathrm{e}^{\bar{\sigma}(\hat{A}+\hat{B}K)h} + \Delta_{\max}(h)\big)r + \big(\mathrm{e}^{\bar{\sigma}(A)h} + \Delta_{\max}(h)\big)\delta \tag{12}$$

where

$$r = \sqrt{\frac{\lambda_{\max}((\mathrm{e}^{Ah} - \Delta(h))^T P(\mathrm{e}^{Ah} - \Delta(h))^T)\delta^2}{\lambda_{\min}(Q_D)}}. \quad \square$$

Remarks: The expressions in Theorem 2 establish a direct relationship between the quantizer density δ, the
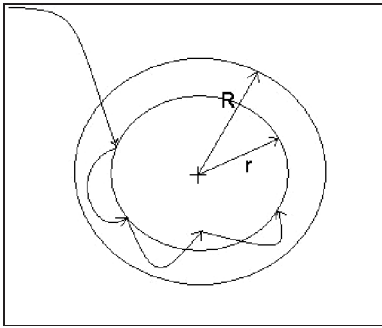
Figure 3. Plant state trajectory.

robustness of the controller characterized by $\lambda_{\min}(Q_D)$, the plant's dynamics, the error between plant and model dynamics, the update time, and the convergence region. Note that the smaller region defined by the radius r is the region where the plant state can be found at each update time, while the larger region R will contain the plant state at all times. In view of the expression for R when the quantization is coarser (δ is larger) R is also larger. Similarly, the larger $\Delta_{\max}(h)$ is, the larger R is. Note that $\Delta_{\max}(h)$ is larger (see (3)) when h is larger, the error between the plant and model is larger; it also depends on the selected control law K. R also depends on r. When $\lambda_{\min}(Q_D)$ is smaller (in view of (2), this is the case for example when the non quantized networked control system is less robustly stable), r is bigger as can be seen from (12).

3.2 State feedback MB-NCS with logarithmic quantization

We will define a logarithmic quantizer as function $q\colon R^n \to R^n$ with the following property:

$$||z - q(z)|| \leq \delta||z||, \ z \in R^n, \ \delta > 0. \tag{13}$$

Theorem 3: *Assume that the networked system without quantization is stable and satisfies*

$$\big(\mathrm{e}^{(\hat{A}+\hat{B}K)^T h} + \Delta(h)^T\big)P\big(\mathrm{e}^{(\hat{A}+\hat{B}K)h} + \Delta(h)\big) - P = -Q_D \tag{14}$$

with P and Q_D symmetric and positive definite. Then when using the logarithmic quantizer defined by (13), *the state feedback MB-NCS is exponentially stable if*

$$\delta < \sqrt{\frac{\lambda_{\min}(Q_D)}{\lambda_{\max}((\mathrm{e}^{Ah} - \Delta(h))^T P(\mathrm{e}^{Ah} - \Delta(h)))}}.$$

Proof: The difference between the values of the plant's state Lyapunov function $V = x^T P x$ at two consecutive update times is given by

$$V(x(t_{k+1})) - V(x(t_k))$$
$$= e_k^T(\mathrm{e}^{Ah} - \Delta(h))^T P(\mathrm{e}^{Ah} - \Delta(h))e_k - x_k^T Q_D x_k. \tag{15}$$

We can now bound (15) using the quantizer property given in (13) by

$$e_k^T(\mathrm{e}^{Ah} - \Delta(h))^T P(\mathrm{e}^{Ah} - \Delta(h))e_k - x_k^T Q_D x_k$$
$$\leq \lambda_{\max}\big((\mathrm{e}^{Ah} - \Delta(h))^T P(\mathrm{e}^{Ah} - \Delta(h))\big)\delta^2||x_k||^2$$
$$- \lambda_{\min}(Q_D)||x_k||^2. \tag{16}$$
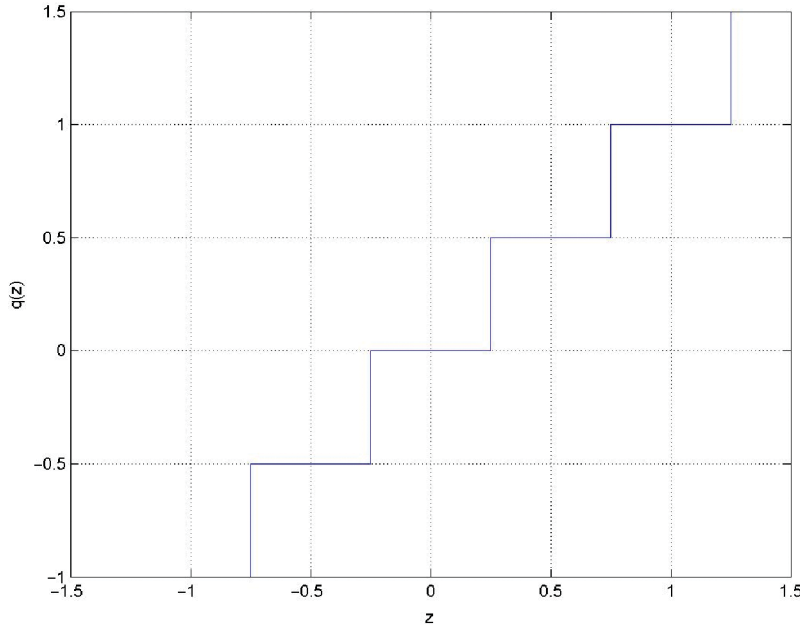
Figure 4.   Uniform quantizer function.

This allows us to ensure exponential stability as in (5) if

$$\lambda_{\max}\big((e^{Ah} - \Delta(h))^T P(e^{Ah} - \Delta(h))\big)\delta^2 - \lambda_{\min}(Q_D) < 0.$$
(17)

Or equivalently (assuming $(e^{Ah} - \Delta(h))^T P(e^{Ah} - \Delta(h)) \neq 0$)

$$\delta < \sqrt{\frac{\lambda_{\min}(Q_D)}{\lambda_{\max}((e^{Ah} - \Delta(h))^T P(e^{Ah} - \Delta(h)))}}$$
(18)

$\square$

Remarks: Theorem 3 relates similar parameters to those in Theorem 2, but logarithmic quantizers can produce an exponentially stable system as opposed to the bounded output obtained with the uniform quantizers. Note that the result states that the maximum logarithmic quantizer's density for stability is reduced if the controlled closed loop system is not robust. This can be seen in (18) where $\lambda_{\min}(Q_D)$ is a measure of robustness.

Example 2:   For this example we will use the following plant model:

$$\dot{\hat{x}} = \begin{bmatrix} 0 & 1 \\ 1 & 3 \end{bmatrix}\hat{x} + \begin{bmatrix} 0 \\ 1 \end{bmatrix}u.$$
(19)

Let the actual plant be a perturbed version of the model, namely:

$$\dot{x} = \begin{bmatrix} -0.0689 & 0.9757 \\ 1.0396 & 3.0720 \end{bmatrix}x + \begin{bmatrix} 0.0707 \\ 1.0187 \end{bmatrix}u.$$
(20)

Both are unstable plants. A stabilizing controller, designed using the plant model, is

$$u = \begin{bmatrix} -2 & -5 \end{bmatrix}\hat{x}.$$
(21)

This controller places both eigenvalues of the compensated plant model at -1. We obtain a stable NCS without quantization for update times less than 1 second.

First we will study the effects of uniform quantization. For this we will use a quantizer that partitions the state space in rectangular regions. The quantizer function for one variable is depicted in figure 4.

This quantizer uses a resolution of 0.1 binary (or 0.5 in decimal notation). The maximum absolute error between the real value of the state and the quantized values is calculated to be $\delta = 0.3536$. By using an update time of $h = 0.2$ seconds and a $Q_D = I$ in equation (2) we obtain a suitable P. We then proceed with (12) to obtain r and R of the region of attraction. The radius R of the region of attraction is calculated to be 2. Figure 5 shows the regions defined by r and R and also the evolution of the plant state when the system is started with an initial condition of $[2\ 2]^T$, figure 6 pictures the plant and model state as a function of time. We note that the actual region of attraction is smaller than the region calculated using Theorem 2, which shows that the result is conservative. Note that conservativeness of the approach is the result of the use of norms and singular values. This can be reduced by traditional
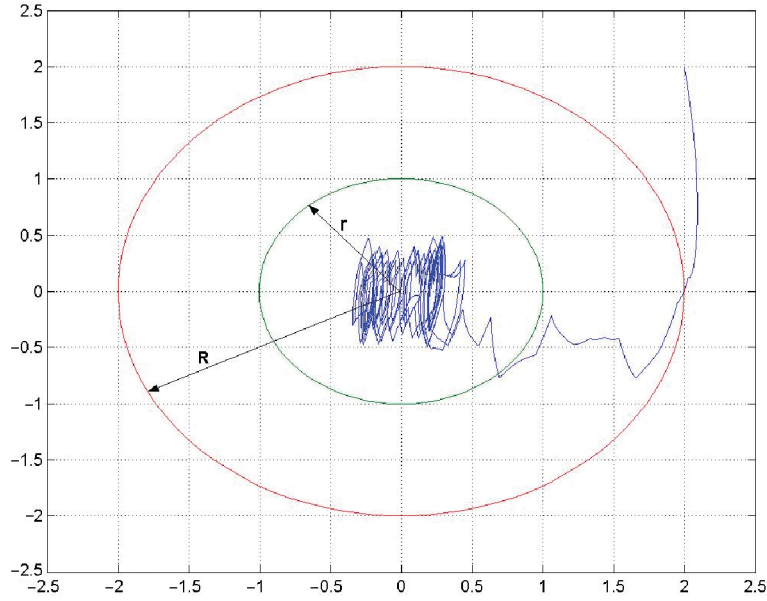
Figure 5. Attraction region and plant state evolution.
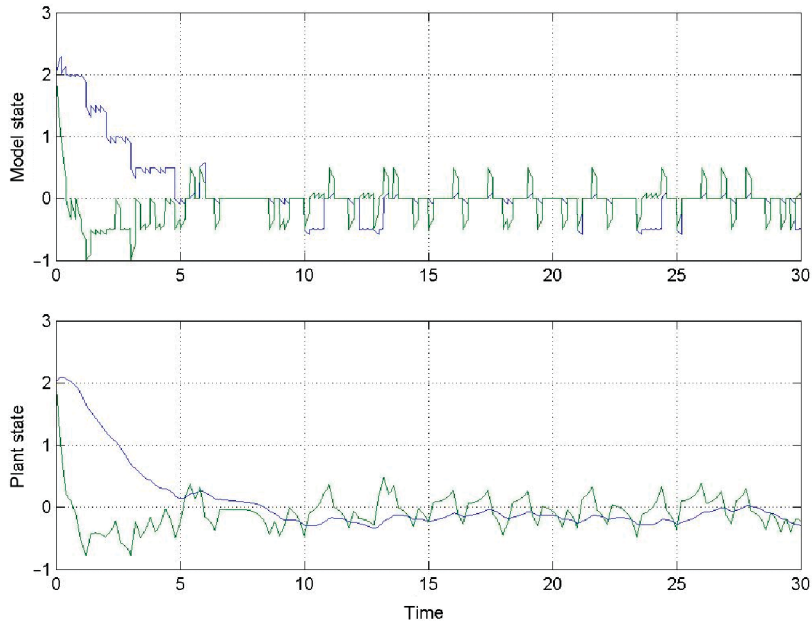
Figure 6. Plant and model state.

diagonalization techniques. The results here presented are meant to relate the different design parameters to the system stability.

We now use the same plant with a logarithmic quantizer and an update time of $h = 0.6$ seconds. We will test two logarithmic quantizer functions: $q1$ with a mantissa word length of 12 bits; and $q2$ with mantissa word length of 13 bits. The functions for one variable are depicted in figure 7.

Their relative errors for the two dimensional case are for $q1$: 0.33 and for $q2$: 0.20. Note that figure 7 shows the quantizer functions on one dimension. When the quantizer is used on vectors the function is applied element wise. We show next the time response of the system for each of the quantizers when the plant state is initialized at $[2\ 3]^T$.

We observe from figures 8 and 9 that the system working with quantizer $q1$ ($\delta = 0.33$) is unstable, while
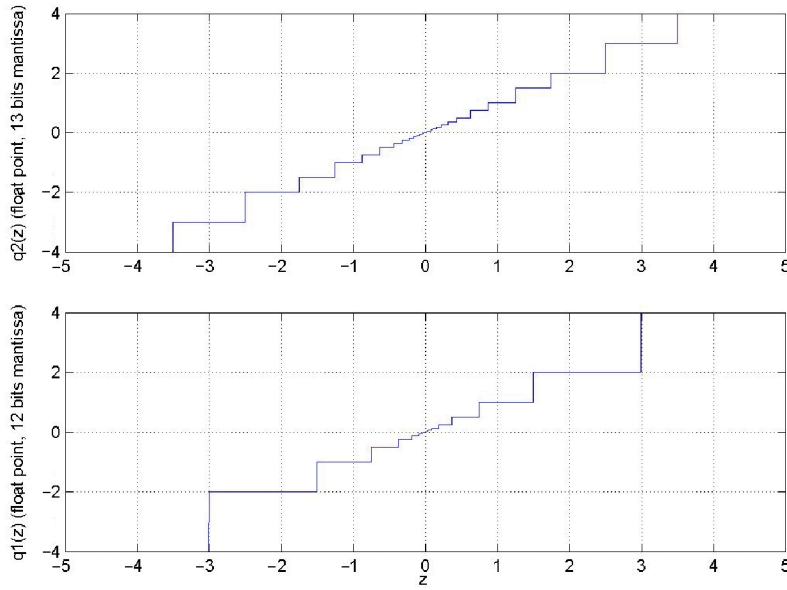
Figure 7.   Quantizer functions.
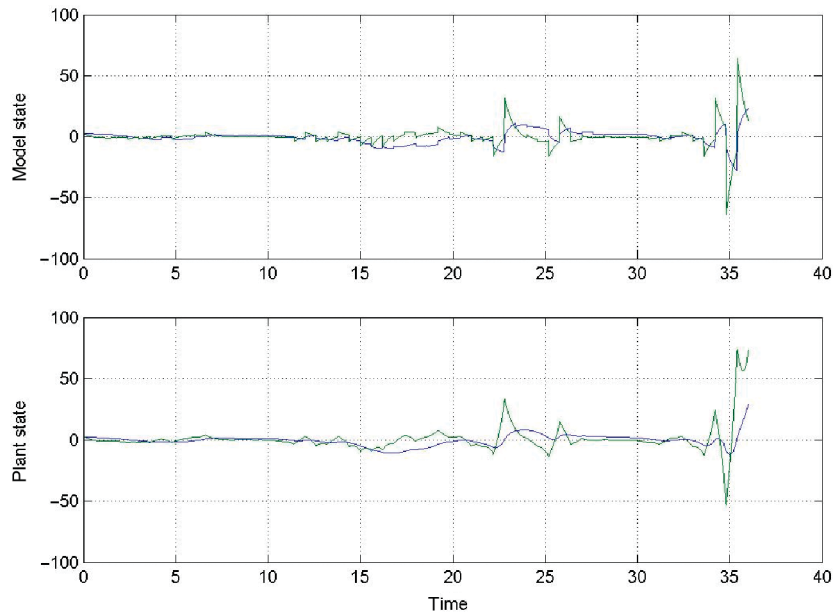
Figure 8.   Plant and Model state time response for $q1$.

with $q1$ ($\delta = 0.20$) is stable. By using Theorem 3 and a $Q_D = I$ we obtain a maximum relative error (18) of 0.1241.

4. Stability of MB-NCS with dynamic quantization

In this section we will consider the case of dynamic quantization, where the quantized region and quantization error vary at each transmission time. It has been shown that these type of quantizers can achieve the smallest bit count per packet while maintaining stability (Nair and Evans 2000a, b, Ling and Lemmon 2004). This comes with the price of increased quantizer complexity. While the static quantizers did require a relatively small amount of computations, the dynamic quantizers need to compute new quantization regions and detect the plant state presence
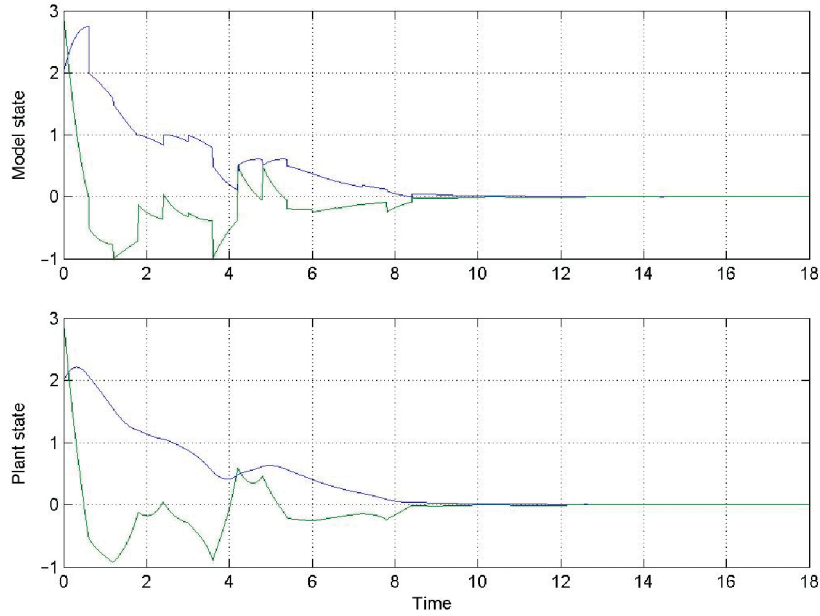
Figure 9. Plant and Model state time response for *q*2.

within each region. Yet dynamic quantizers are an attractive alternative when the number of bits available per transmission is restricted. Our results extend those already available in the literature to the case of MB-NCS. It will be shown that our results converge to existing standard literature results when the model uncertainty is zero.

Under the dynamic quantizer scheme, an encoder measures the state of the plant at each transmission time and sends a symbol to the decoder collocated with the plant model. To do so, first the encoder and decoder assume that the plant state is contained in a hyper-parallelogram R_k. Next, the encoder uses the plant model and plant-model uncertainties to determine the region where the plant state is at the next transmission time. This calculated region will also be a hyper-parallelogram denoted as R_{k+1}^-. The encoder can also calculate R_{k+1}^- since its calculation is based on the plant model dynamics and known uncertainty bounds. Then, the encoder can divide R_{k+1}^- in 2^N smaller equal hyper-parallelograms. N is an integer representing the number of bits used to identify each smaller parallelogram. The encoder then sends an N-bit symbol representing the smaller parallelogram R_{k+1} within R_{k+1}^- where the plant state is. The process can be repeated.

We will assume that the plant model matrix $\hat{A}$ has distinct real unstable eigenvalues. This assumption can be relaxed at the expense of more complex notation and problem geometry. We will also assume that the compensated model is stable.

Previous results (Hespanha *et al.* 2002, Ling and Lemmon 2004) consider a similar case but our result

is novel in that it incorporates the plant-model mismatch within our MB-NCS approach. Ling and Lemmon (2004) calculate the minimum bit rate for NCS under network dropouts. Hespanha *et al.* (2002), consider the case of a NCS that incorporates an exact model of the plant. The results in Hespanha *et al.* (2002) yield the minimum bit rate for stabilizing the NCS under bounded measurement noise and input disturbance. A similar method that does not consider uncertainty or model-based techniques is used in Ling and Lemmon (2004) called the uncertain set evolution method. Namely, at transmission time t_k, the encoder partitions the hyper-parallelogram R_k^-, containing the plant state $x(t_k)$ into 2^N smaller hyper-parallelograms and sends the decoder the symbol identifying the partition R_k that contains the plant state. The controller then uses the center c_k of R_k to update the plant model generates the control signal using the plant model until time t_{k+1}^-. At this point, both encoder and decoder calculate a new hyper-parallelogram R_{k+1}^- that should contain the plant state by evolving or propagating forward the initial region R_k. The process is then repeated. Stability will be ensured if the radius and center of the hyper-parallelograms converge to zero with time. We will show now how the hyper-parallelogram R_{k+1}^- is obtained from R_k.

Assume that the plant model matrix $\hat{A} \in R^{n \times n}$ has n distinct unstable eigenvalues $\lambda_1, \lambda_2, \ldots, \lambda_n$ with n corresponding linearly independent normalized eigenvectors $v_1, v_2, \ldots, v_n \in R^n$. We will also assume that at $t = 0$ both encoder and decoder agree upon a hyper-parallelogram R_0 containing the initial state

of the plant. Denote a hyper-parallelogram as the $(n+1)$-tuple where c is the center of the hyper-parallelogram and η_i are its axis. In particular

$$R(c, \eta_1, \eta_2, \ldots, \eta_n) = \left\{ x \in R^n, \sum_{i=1}^{n} \alpha_i \eta_i = x - c, \right.$$
$$\text{where } \eta_i \in R^n, \alpha_i \in [-1, 1],$$
$$\left. \text{and } c \in R^n \right\}.$$

Let each hyper-parallelogram R_k with center c_k be defined as follows:

$$R_K = R(c_k, \eta_{k,1}, \eta_{k,2}, \ldots, \eta_{k,n}) \tag{22}$$

where

$$\eta_{k,i} = b_{k,i} v_i \quad \text{and} \quad b_{k,i} \in R.$$

Therefore it can be easily verified that according to the plant dynamics the region R_k evolves into a hyper-parallelogram R_{k+1}^p defined by

$$R_{k+1}^p = R\left(c_{k+1}^p, \eta_{k+1,1}^p, \eta_{k+1,2}^p, \ldots, \eta_{k+1,n}^p\right)$$
$$\text{with } \eta_{k+1,i}^p = e^{Ah}\eta_{k,i} \tag{23a}$$

and

$$c_{k+1}^p = \left(e^{Ah} + \int_0^h e^{A(h-s)} BK e^{(\hat{A}+\hat{B}K)s} ds\right) c_k. \tag{23b}$$

Correspondingly, according to the plant model dynamics the hyper-parallelogram R_k should evolve into a different hyper-parallelogram R_{k+1}^m

$$R_{k+1}^m = R\left(c_{k+1}^m, \eta_{k+1,1}^m, \eta_{k+1,2}^m, \ldots, \eta_{k+1,n}^m\right)$$
$$\text{with } \eta_{k+1,i}^m = e^{\lambda_i h}\eta_{k,i}, \tag{24}$$
$$\text{and } c_{k+1}^m = e^{(\hat{A}+\hat{B}K)h} c_k.$$

According to equation (24) the hyper-parallelogram R_{k+1}^m has edges that are parallel to those of the original hyper-parallelogram R_k but are longer by a factor of $e^{\lambda_i h}$ for each corresponding edge. Also the center of the parallelogram has shifted. Note that the hyper-parallelogram R_{k+1}^m doesnot necessarily contain the plant state. We will now express R_{k+1}^p in terms of the parameters of R_{k+1}^m. By replacing h by t and using

Laplace transforms the expressions in (23) can be easily manipulated

$$e^{Ah} \xrightarrow{L} (sI - A)^{-1}$$
$$= (sI - A)^{-1}(sI - \hat{A})(sI - \hat{A})^{-1}$$
$$= (I + (sI - A)^{-1}\tilde{A})(sI - \hat{A})^{-1}$$
$$= (sI - \hat{A})^{-1} + (sI - A)^{-1}\tilde{A}(sI - \hat{A})^{-1}$$
$$\xrightarrow{L^{-1}} e^{\hat{A}h} + \int_0^h e^{A(h-s)}\tilde{A}e^{\hat{A}s} ds$$

and

$$e^{Ah} + \int_0^h e^{A(h-s)} BK e^{(\hat{A}+\hat{B}K)s} ds$$
$$\xrightarrow{L} (sI - A)^{-1} + (sI - A)^{-1} BK(sI - (\hat{A} + \hat{B}K))^{-1}$$
$$= (sI - A)^{-1}(sI - \hat{A} + \tilde{B}K)(sI - (\hat{A} + \hat{B}K))^{-1}$$
$$= (sI - (\hat{A} + \hat{B}K))^{-1} + (sI - A)^{-1}(\tilde{A} + \tilde{B}K)$$
$$\times (sI - (\hat{A} - \hat{B}K))^{-1}$$
$$\xrightarrow{L^{-1}} e^{(\hat{A}+\hat{B}K)h} + \int_0^h e^{A(h-s)}(\tilde{A} + \tilde{B}K)e^{(\hat{A}+\hat{B}K)s} ds. \tag{25}$$

Therefore the parameters of R_{k+1}^p can be expressed in terms of the parameters of R_{k+1}^m

$$\eta_{k+1,i}^p = e^{Ah}\eta_{k,i} = \left(e^{\hat{A}h} + \int_0^h e^{A(h-s)}\tilde{A}e^{\hat{A}s} ds\right)\eta_{k,i}$$
$$= e^{\hat{A}h} b_{k,i} v_i + \left(\int_0^h e^{A(h-s)}\tilde{A}e^{\hat{A}s} ds\right)\eta_{k,i}$$
$$= e^{\lambda_i h}\eta_{k,i} + \Delta_\eta(h)\eta_{k,i}$$
$$= \eta_{k+1,i}^m + \Delta_\eta(h)\eta_{k,i}$$
$$c_{k+1}^p = \left(e^{Ah} + \int_0^h e^{A(h-s)} BK e^{(\hat{A}+\hat{B}K)s} ds\right)$$
$$c_k = \left(e^{(\hat{A}+\hat{B}K)h} + \int_0^h e^{A(h-s)}(\tilde{A} + \tilde{B}K)e^{(\hat{A}+\hat{B}K)s} ds\right) c_k$$
$$= e^{(\hat{A}+\hat{B}K)h} c_k + \left(\int_0^h e^{A(h-s)}(\tilde{A} + \tilde{B}K)e^{(\hat{A}+\hat{B}K)s} ds\right) c_k$$
$$= c_{k+1}^m + \Delta_c(h)c_k. \tag{26}$$

Note that the matrices $\Delta_c(h)$ and $\Delta_\eta(h)$ can be calculated as follows:

$$\Delta_c(h) = [I \quad 0] e^{\left(\begin{bmatrix} A & \tilde{A}+\tilde{B}K \\ 0 & \hat{A}+\hat{B}K \end{bmatrix} h\right)} \begin{bmatrix} 0 \\ I \end{bmatrix},$$

$$\Delta_\eta(h) = [I \quad 0] e^{\left(\begin{bmatrix} A & \tilde{A} \\ 0 & \hat{A} \end{bmatrix} h\right)} \begin{bmatrix} 0 \\ I \end{bmatrix}. \tag{27}$$
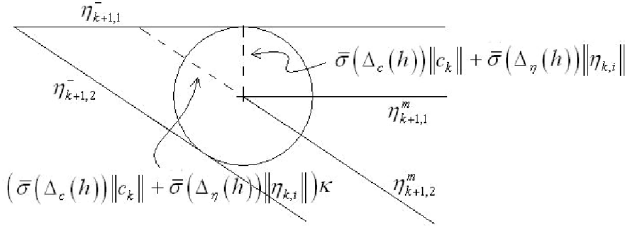
Figure 10. Construction of hyper-parallelogram R_{k+1}^{-} from R_{k+1}^{m}.

Figure 11. Evolution of quantized regions.

Since matrices $\Delta_c(h)$ and $\Delta_\eta(h)$ are unknown, the hyper-parallelogram R_{k+1}^{p} cannot be constructed. Instead we will use the expressions in equation (26) and the bounds over the norms of $\Delta_c(h)$ and $\Delta_\eta(h)$ to construct a hyper-parallelogram that will contain the plant state, i.e., it will contain R_{k+1}^{p}. This is depicted in figure 10.

$$R_{k+1}^{-} = R\left(c_{k+1}^{-}, \eta_{k+1,1}^{-}, \eta_{k+1,2}^{-}, \ldots, \eta_{k+1,n}^{-}\right)$$

with $\eta_{k+1,i}^{-} = \left(1 + \bar{\sigma}(\Delta_c(h))||c_k|| \dfrac{\kappa}{||\eta_{k+1,i}^{m}||}\right.$

$$\left. + \bar{\sigma}(\Delta_\eta(h))||\eta_{k,i}|| \dfrac{\kappa}{||\eta_{k+1,i}^{m}||}\right)\eta_{k+1,i}^{m}$$

and $c_{k+1}^{-} = c_{k+1}^{m}$, $\qquad$ (28)

where

$$\kappa = 1/\det([v_1 v_2 \ldots v_n]), \quad ||v_i|| = 1.$$

Note that bounds over $\bar{\sigma}(\Delta_c(h))$ and $\bar{\sigma}(\Delta_\eta(h))$ can be obtained based on the norms over the error matrices $\tilde{A}$ and $\tilde{B}$. Note also that R_{k+1}^{-} is a hyper-parallelogram with edges larger but parallel to those of R_{k+1}^{m}. At this time the encoder will divide R_{k+1}^{-} into smaller parallelograms and transmits to the decoder the symbol that identifies the one that contains the plant state R_{k+1}. And the process repeats itself again. This process is depicted below, also see figure 11

$$R_k^{-} \xrightarrow{\text{encoder}} R_k \xrightarrow[\text{h seconds}]{\text{plant}} R_{k+1}^{-} \xrightarrow{\text{encoder}} R_{k+1}. \qquad (29)$$

In figure 11 the term d_k represents the displacement of the center of R_{k+1} with respect to the center of R_{k+1}^{-}. We will now establish the relationship between the evolution of the hyper-parallelograms parameters and stability. Define the radius of the hyper-parallelogram R_k with center c_k

$$\lambda_{\max}(R_k) = \sup_{x \in R_k} ||x - c_k||. \qquad (30)$$

It is clear that in order to ensure the stability of the system we require that the center and radius of the hyper-parallelograms must converge to zero with time. As a matter of fact, for stability, only the radius of the hyper-parallelograms R_k is relevant. This is stated in Theorem 4.

Theorem 4: *Assume that state feedback NCS without quantization is asymptotically stable then the NCS with dynamical quantization is asymptotically stable if and only if*

$$\lim_{k \to \infty} \lambda_{\max}(R_k) = 0. \qquad (31)$$

Proof: *Sufficiency*: We know that $\lim_{k \to \infty} \lambda_{\max}(R_k) = 0$ implies that the quantization error at each sampling time also converges to zero: $\lim_{k \to \infty} e(t_k) = 0$. Also, it can be proved, as in equation (4), that

$$x(t_{k+1}) = x(t_{k+1}^{-})$$
$$= \left(e^{(\hat{A}+\hat{B}K)h} + \Delta_c(h)\right)x(t_k) + (e^{Ah} - \Delta_c(h))e(t_k)$$
$$= Mx(t_k) + Ne(t_k). \qquad (32)$$

Since the NCS without quantization is stable the matrix M is Schur stable, therefore is it is clear that if the quantization error converges to zero then the sequence of states $x(t_k)$ also converges to zero. Note that since the plant is an LTI plant, the fact that the sequence $x(t_k)$ converges to zero ensures that plant state will also converge to zero.

Necessity: In order to ensure that there is no non zero sequence of $e(k)$ that can drive the plant state to zero and keep it there we just need to prove that the matrix N has full rank. This is readily observed from the way N can be computed

$$N = e^{Ah} - \Delta_c(h) = [I \quad 0]e^{\begin{bmatrix} A & \tilde{A}+\tilde{B}K \\ 0 & \hat{A}+\hat{B}K \end{bmatrix}h}\begin{bmatrix} I \\ I \end{bmatrix}. \qquad (33)$$

From equation (33) it can be observed that the left most matrix isolates the two upper blocks of the exponential,

since the exponential matrix has rank $2n$, the isolated matrix (of size $n \times 2n$) should have rank n. Therefore, any non zero error vector multiplied by N will yield a non zero vector. $\qquad\square$

Remarks: Assume that in order to generate the hyper-parallelograms R_{k+1} each edge of the hyper-parallelogram R_{k+1}^- is divided in equal Q_i parts. Note that all the Q_i must be powers of 2, that is $Q_i = 2^{b_i}$ where b_i represent the number of bits assigned to each axis. The resulting bit rate is $BitRate = \left(\sum_{i=1}^{n} b_i\right)/H$. We can now present a sufficient condition for stability of MB-NCS under the described dynamic quantization.

Theorem 5: *The state feedback MB-NCS using the dynamic quantization described in* (29) *is globally asymptotically stable if the following conditions are satisfied*:

(1) *The non-quantized MB-NCS is stable.*
(2) *The test matrix T has all its eigenvalues inside the unit circle.*

where

$$T = \begin{bmatrix} T_{11a} + T_{11b} & T_{12} \\ T_{21} & T_{22} \end{bmatrix}$$

with $T_{11a} = \mathrm{diag}\left(\left(\dfrac{e^{\lambda_1 h} + \bar{\sigma}(\Delta_\eta(h))\kappa}{Q_1}\right),\right.$

$$\left. \dots, \left(\dfrac{e^{\lambda_n h} + \bar{\sigma}(\Delta_\eta(h))\kappa}{Q_n}\right)\right),$$

$$T_{11b} = \begin{bmatrix} \left(\dfrac{Q_1 - 1}{Q_1}\right) & \cdots & \left(\dfrac{Q_n - 1}{Q_n}\right) \\ \vdots & & \vdots \\ \left(\dfrac{Q_1 - 1}{Q_1}\right) & \cdots & \left(\dfrac{Q_n - 1}{Q_n}\right) \end{bmatrix} \bar{\sigma}(\Delta_c(h))\kappa,$$

$$T_{12} = \begin{bmatrix} \bar{\sigma}(\Delta_c(h))\kappa \\ \vdots \\ \bar{\sigma}(\Delta_c(h))\kappa \end{bmatrix},$$

$$T_{21}{}^{\text{`}} = \begin{bmatrix} \left(\dfrac{Q_1 - 1}{Q_1}\right) & \cdots & \left(\dfrac{Q_n - 1}{Q_n}\right) \end{bmatrix} \bar{\sigma}\left(e^{(\hat{A} + \hat{B}K)h}\right),$$

$$T_{22} = \bar{\sigma}(e^{(\hat{A} + \hat{B}K)h}) \tag{34}$$

Proof: In order to characterize the evolution of the hyper-parallelograms it is convenient to establish the relationship between the sizes of edges of R_{k+1}^- and the edges of R_k^-

$$\left\|\eta_{k+1, i}^-\right\| = \left(\dfrac{e^{\lambda_i h} + \bar{\sigma}(\Delta_\eta(h))\kappa}{Q_i}\right)\left\|\eta_{k, i}^-\right\| + \bar{\sigma}(\Delta_c(h))\kappa\|c_k\|$$

$$\leq \left(\dfrac{e^{\lambda_i h} + \bar{\sigma}(\Delta_\eta(h))\kappa}{Q_i}\right)\left\|\eta_{k, i}^-\right\|$$

$$+ \bar{\sigma}(\Delta_c(h))\kappa\left\|c_k^-\right\| + \bar{\sigma}(\Delta_c(h))\kappa\|d_k\|. \tag{35}$$

Equation (35) is a scalar discrete linear system. It is dependent on $\left\|c_k^-\right\|$. The evolution of c_k is given below

$$c_{k+1}^- = e^{(\hat{A} + \hat{B}K)h}c_k = e^{(\hat{A} + \hat{B}K)h}c_k^- + e^{(\hat{A} + \hat{B}K)h}d_k. \tag{36}$$

The term $\|d_k\|$ is bounded by

$$\|d_k\| \leq \sum_{i=1}^{N}\left(\left\|\eta_{k+1, i}^-\right\|\left(\dfrac{Q_i - 1}{Q_i}\right)\right). \tag{37}$$

We will now bound $\|c_k^-\|$

$$\left\|c_{k+1}^-\right\| \leq \bar{\sigma}\left(e^{(\hat{A} + \hat{B}K)h}\right)\|c_k^-\|$$

$$+ \bar{\sigma}\left(e^{(\hat{A} + \hat{B}K)h}\right)\sum_{i=1}^{N}\left(\left\|\eta_{k+1, i}^-\right\|\left(\dfrac{Q_i - 1}{Q_i}\right)\right). \tag{38}$$

From (35), (37) and (38) it is clear that stability is guaranteed if T has its eigenvalues inside the unit circle.

Remarks: Note that if the plant model is exact, $\tilde{A} = 0$ and $\tilde{B} = 0$, then $\Delta_c(h) = 0$ and $\Delta_\eta(h) = 0$. This implies that if $\bar{\sigma}(e^{(\hat{A} + \hat{B}K)h}) < 1$ then stability is guaranteed provided that $\max_i(e^{\lambda_i h}/Q_i) < 1$ which is a well-established result (Nair and Evans 2000a, b). In order to enforce the condition that $\bar{\sigma}(e^{(\hat{A} + \hat{B}K)h}) < 1$ it is convenient to apply a similarity transformation that diagonalizes $\hat{A} + \hat{B}K$. In order to obtain a value of $\bar{\sigma}(e^{(\hat{A} + \hat{B}K)h})$ that is close to the magnitude of the maximum eigenvalue of $e^{(\hat{A} + \hat{B}K)h}$.

Next an example is presented, This example depicts the way a MB-NCS can be designed, namely first a non-quantized MB-NCS is designed and then a suitable quantization scheme is added and tested for stability.

Example 3: Consider the plant described by the following matrices:

$$A = \begin{bmatrix} 0 & 1 \\ a_{21} & 0.5 \end{bmatrix} \quad B = \begin{bmatrix} 0.1 \\ 0.2 \end{bmatrix}, \tag{39}$$

where $a_{11} \in [-0.01, \ 0.01]$ represents the uncertainty in the A matrix. Let the plant model be the nominal plant, that is

$$\hat{A} = \begin{bmatrix} 0 & 1 \\ 0 & 0.5 \end{bmatrix} \quad \hat{B} = \begin{bmatrix} 0.1 \\ 0.2 \end{bmatrix}. \tag{40}$$

A feedback gain $K = [-3.3333 \ -8.3333]$ is selected so to place the eigenvalues of the plant model at $(-0.5, -1)$. An update time of $h = 1\,\text{sec}$ is used. To reduce conservativeness, the following similarity transformation that diagonalizes $\hat{A} + \hat{B}K$ is applied to the system

$$x_{\text{new}} = Px, \text{ where } P = \begin{bmatrix} 1.8856 & 0.4714 \\ 1.3744 & 1.3744 \end{bmatrix}. \tag{41}$$

Finally, the quantized levels are defined as $n_1 = 1$ bit and $n_2 = 2$ bits for the eigenvectors corresponding to the

eigenvalues at -0.5 and -1 respectively. Note the need for more bits for faster eigenvalues. The bounds for the norms of the uncertainty matrices are calculated in the transformed space by searching along the parameter a_{21}; they are as follows:

$$\bar{\sigma}(\Delta_c(h)) \le 0.1354, \quad \bar{\sigma}(\Delta_\eta(h)) \le 0.0961 \qquad (42)$$

The maximum eigenvalue for the test matrix T is 0.9531 indicating that the quantized system is stable. Next a simulation of the system is presented. In this simulation the parameter a_{21} is chosen to be 0.0034, the starting region to have a center $[2\text{--}3]^T$, with edges of length 1; the plant state is placed randomly within this region. The plots are in the non-transformed original space (figures 12–14).

In this example we use a simple plant and controller to show how the design technique is used. Note that the complexity of the calculations involved depends on the number of states in the plant. Note that the
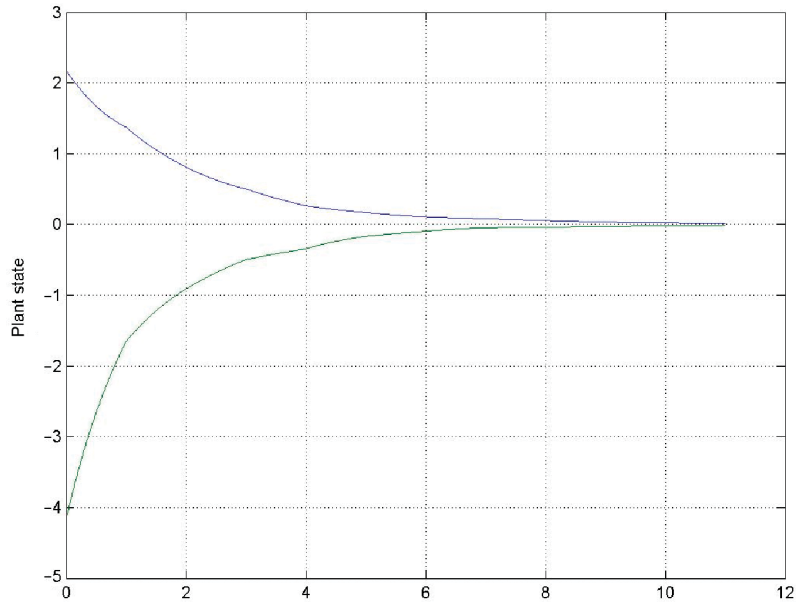
Figure 12. Plant state.
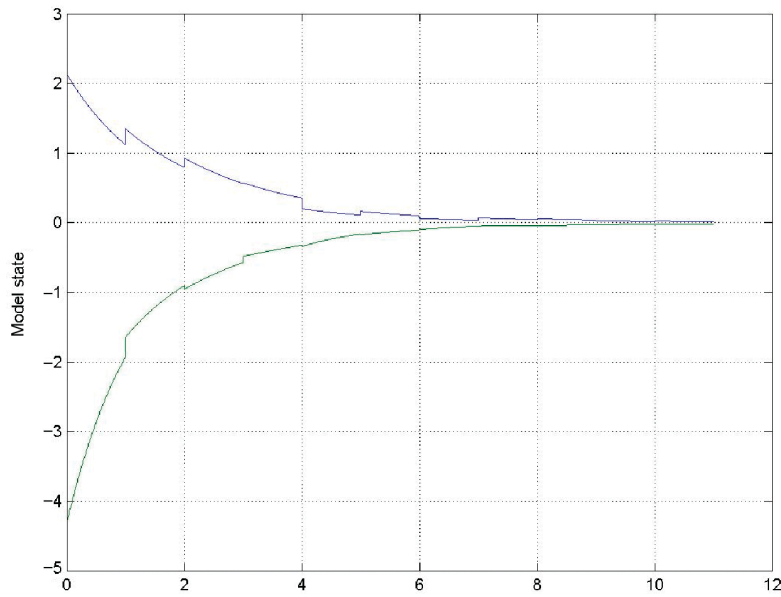
Figure 13. Plant model state.
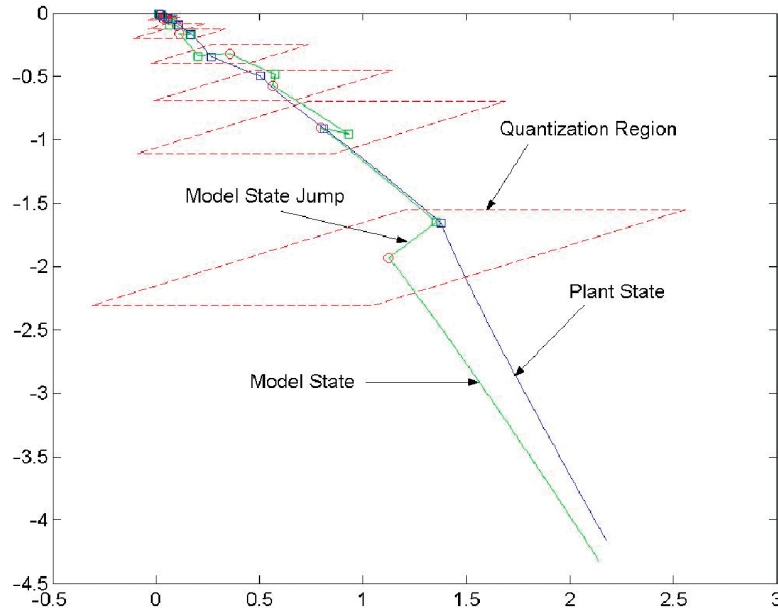
Figure 14. Trajectories for plant state and plant model state showing the evolution of quantized regions.

calculations used to determine the stability of a particular system are performed off-line. In contrast the calculations used to quantize the plant state vector are done on-line. For these on-line calculations, the proposed scheme carries a similar computational intensity to that of dynamic quantizers without MB-NCS with the addition of the computations shown in (28) and the model simulation.

5. Conclusions

Sufficient conditions for the stability of quantized MB-NCS were presented. These results consider three different types of quantizers. The quantizers studied relate to popular data representation models. In particular, the uniform quantizer is related to fixed-point number representations, while the logarithmic quantizer is related to the floating-point representation. The results although conservative provide a way to relate the effects of uncertainty, model update times, and non-networked control robustness to system stability. A third more complex quantizer based on traditional dynamic quantization was also introduced; the dynamic quantizer uses an integral representation of the data in an adaptive manner. That is, the data transmitted represents an area within a region where the state of the plant is known to be. The regions evolve according to plant model and the uncertainties bound over the model parameters. It was shown that if the uncertainties are eliminated, the minimum data rate needed for stability coincides with the well-known minimal theoretical rate for stability (Nair and Evans 2000a).

While the computations required to verify stability can be complex, the calculations performed by the quantizer are similar in nature to those performed by dynamic quantizers that do not consider uncertainty. An important feature of the paper is that the results show explicitly the dependence on several design parameters such as modelling error, quantization parameters, measures of robustness.

References

B. Bamieh, "Intersample and finite wordlength effects in sampled-data problems", in *Proc. of the 35th IEEE Conf. on Dec. and Cont.*, Kobe, Japan, December 1996, pp. 3890–3895.

N. Elia and S. Mitter, "Stabilization of linear systems with limited information", *IEEE Trans. Auto. Contr.*, 46, pp. 1384–1400, 2001.

F. Fagnani and S. Zampieri, "Stabilizing quantized feedback with minimal information flow: the scalar case", *15th International Symposium on Mathematical Theory of Networks and Systems*, Notre Dame, IN, USA, 2002.

M. Fu, "Robust stabilization of linear uncertain systems via quantized feedback", in *Proc. of the 42nd IEEE Conf. on Dec. and Con.*, Maui, Hawaii USA, December 2003, pp. 199–203.

J. Hespanha, A. Ortega and L. Vasudevan, "Towards the control of linear systems: with minimum bit-rate", in *Proc. of the 15th Int. Symposium on Mathematical Theory of Networks and Sys.*, Notre Dame, IN, USA, August 2002.

D. Liberzon and R. Brockett, "Quantized feedback stabilization of linear systems", *IEEE Trans. Auto. Cont.*, 45, pp. 1279–1289, 2000.

D. Liberzon, "Hybrid feedback stabilization of systems with quantized signals", *Automatica*, 39, pp. 1543–1554, 2003a.

D. Liberzon, "On stabilization of linear systems with limited information", *IEEE Trans. Auto. Contr.*, 48, pp. 304–307, 2003b.

D. Liberzon, "Stabilizing a nonlinear system with limited information feedback", in *Proc. of the 42nd IEEE Conf. on Dec. and Cont.*, Maui, Hawaii USA, December 2003c, pp. 182–186.

Q. Ling and M.D. Lemmon, "Stability of quantized control systems under dynamic bit assignment", in *Proc. of the 2004 American Cont. Conf.*, Boston, MA, pp. 4915–4920, 2004.

L.A. Montestruque and P.J. Antsaklis, "Model-based networked control systems: necessary and sufficient conditions for stability", *10th Mediterranean Conf. on Cont. and Automation*, Las Vegas, NV, USA, pp. 1620–1625, July 2002a.

L.A. Montestruque and P.J. Antsaklis, "State and output feedback control in model-based networked control systems", *41st IEEE Conf. on Dec. and Cont.*, December 2002b.

L.A. Montestruque and P.J. Antsaklis, "On the model-based control of networked systems", *Automatica*, 39, pp. 1837–1843, 2003.

L.A. Montestruque and P.J. Antsaklis, "Stability of networked control systems with time-varying transmission times", *Transact. Auto. Cont.*, 49, pp. 1562–1572, 2004.

L.A. Montestruque, "Model-based networked control systems". PhD thesis, University of Notre Dame (2004).

G. Nair and R. Evans, "Stabilization with data-rate-limited feedback: tightest attainable bounds", *Syst. Contr. Lett.*, 41, pp. 49–56, 2000a.

G. Nair and R. Evans, "Communication-limited stabilization of linear systems," *Proc. of the Conf. on Dec. and Cont.*, Sydney, Australia, 2000b, pp. 1005–1010.

G. Nair, S. Dey and R. Evans, "Infimum data rates for stabilising markov jump linear systems", in *Proc. of the 42nd IEEE Conf. on Dec. and Cont*, Maui, Hawaii, 2003, pp. 1176–1181.

Networked Control Systems Sessions, in *Proceedings of Conference on Decision and Control & Proceedings of American Control Conference*, starting in 2003.

J.K. Yook, D.M. Tilbury and N.R. Soparkar, "Trading computation for bandwidth: reducing communication in distributed control Systems using State Estimators", *IEEE Transact. Contr. Syst. Technol.*, 10, pp. 503–518, 2002.

G. Walsh, H. Ye and L. Bushnell, "Stability analysis of networked control systems", in *Proc. of American Con. Conf.*, San Diego, CA, USA, June 1999.

H. Ye, A.N. Michel and L. Hou, "Stability analysis of systems with impulse effects", *IEEE Transact. Automat. Contr.*, 43, pp. 1719–1723, 1998.